VACUUM SYSTEM FOR THE DIAMOND LIGHT SOURCE DDBA UPGRADE

M.P. Cox[†], M.J. Duignan, R. Howard, S.C. Lay, A.G. Miller, H.S. Shiers, A.J. Wolfenden,
Diamond Light Source, Didcot, UK

Abstract

One cell of the Diamond Light Source (Diamond) storage ring was upgraded in late 2016 to a Double Double Bend Achromat (DDBA) configuration to provide an additional mid-achromat insertion device straight. For practical reasons it was decided to use discrete non-evaporable getter (NEG) pumps rather than NEG coatings. This paper outlines the vacuum design of the upgrade, the reasons for the choices made and the vacuum simulation tools used as well as describing the vacuum system engineering, assembly, installation and commissioning. The measured vacuum performance is found to be in close agreement with the simulations and a simple expression is derived for the beam gas lifetime.

INTRODUCTION

The motivation for, and general concept of, the Diamond DDBA upgrade have been described elsewhere [1]. The upgrade required the vacuum system for a whole 17.35 m achromat to be replaced with a new, lower aperture design. The design goal was to achieve an average pressure along the electron beam path in the 10^{-9} mbar range at an operating current of 300 mA after a reasonable period of beam condition of order of 100 A.h. Installation and commissioning had to be completed within a scheduled 8-week machine shutdown.

VACUUM PUMPING DESIGN

The new DDBA vessel internal cross section is generally a 27 × 18 mm ellipse compared with typical 80 × 40 mm octagon of Diamond's existing double bend achromat (DBA) sections. The DDBA vacuum system is therefore much more strongly conductance limited than the existing design.

Consequently, vacuum design studies initially focussed on a fully-NEG-coated solution to provide low outgassing rates and high local pumping speed, as implemented, for example, in the Max IV 3 GeV storage ring [2]. These initial studies indicated a fully-NEG-coated solution could deliver a dynamic pressure of 10^{-9} mbar at 300 mA after only 9 A.h of beam conditioning. In practice, beam conditioning would most likely have taken somewhat longer that this, as the simulation did not fully consider scattered radiation.

A fully-NEG-coated solution, however, would have involved a significant amount of R&D work to develop reliable coating parameters and procedures for 21 different vacuum vessels and assemblies. This seemed a disproportionate amount of effort for upgrading only one cell, so an alternative solution without NEG coating was explored and subsequently adopted.

As shown in Figure 1, the chosen pumping scheme was to fit 7 compact NEG cartridge pumps [3] at optimised locations along the beam path, in the small available spaces between the magnets, supplemented by 3 sputter ion pumps (SIPs) at crotch absorbers downstream of dipoles 1, 3 and 4. X-rays are extracted externally at crotches 1 and 3 only. There was no space for a crotch absorber and SIP downstream of dipole 2 and, as there was no requirement to extract x-rays at that point, the crotch was omitted, the synchrotron radiation (SR) from the dipole being mainly captured on the cooled wall of the curved, elliptical cross-section, copper dipole vessel. Although not ideal for vacuum pumping, this proved acceptable, as in addition to the NEG cartridge pumps, a high SIP pumping speed of 1500 l/s was present nearby in the new mid-achromat in-vacuum undulator.
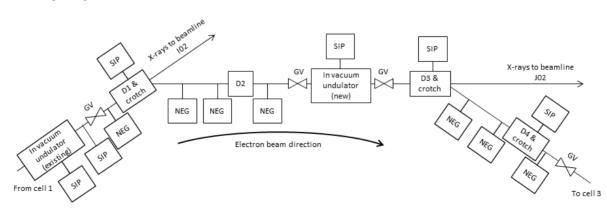

Figure 1: Vacuum pumping layout. NEG=NEG Cartridge Pump, SIP=Sputter Ion Pump, D=Dipole Magnet, GV=RF Shielded Gate Valve. Dipole bend angles have been adjusted for clarity.

VACUUM SIMULATIONS

Vacuum simulations were carried out for the 4 main residual gases H_2, CO, CO_2 and CH_4 using the 1-d "Pressure Profile" code [4]. Molecular gas flows in the geometrically-complex areas such as the pumping grilles for the NEG cartridge pumps were pre-modelled using the full 3-d angular coefficients method [5] and the parameters so obtained were used as inputs to the 1-d calculations. Published values were used for thermal outgassing rates and photon stimulated desorption (PSD) yields [6]. Geometrical ray tracing was used to obtain the photon distribution on the absorbers and vessel walls, from which the surface photon dose and PSD gas load were calculated.
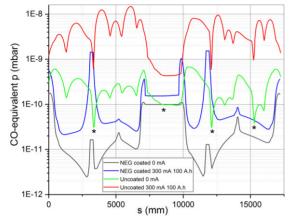

Figure 2: Simulated dynamic and static CO-equivalent pressure along the electron beam path for NEG-coated and uncoated options.

Figure 2 shows the calculated pressure (CO-equivalent pressure) vs distance s along the electron beam path for both dynamic (with stored beam) and static (without stored beam) cases and with and without NEG coating. The CO-equivalent pressure was calculated as a Z^2 weighted sum of the individual partial pressures. The predicted pressure for the NEG-coated option is generally 1 to 2 orders of magnitude lower than for the uncoated option; as expected, near the SIPs (indicated with * in Figure 2) the NEG coating has less effect.
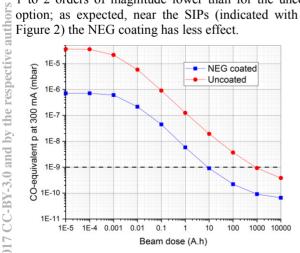

Figure 3: Simulated beam conditioning curve for NEG coated and uncoated designs.

Figure 3 shows the simulated beam conditioning curves for the NEG-coated and uncoated options. The NEG-coated design, requires only 9 A.h to achieve a 300 mA dynamic pressure of 10^{-9} mbar, and has much better vacuum performance than the uncoated design which requires 900 A.h to achieve the same dynamic pressure. However, as only one cell was being upgraded to DDBA, the vacuum performance of the uncoated design was accepted and adopted for the practical reasons mentioned above.

VACUUM ENGINEERING

Vessels were constructed from 316L stainless steel and OFS copper with 316LN flanges. Copper was used where higher thermal conductivity was needed while stainless steel was used in areas needing higher mechanical strength or lower electrical conductivity (in regions of AC magnets).

In addition to the discrete photon absorbers at 3 of the crotches, the SR heat load was handled by distributed water-cooled absorbers along the vessel walls with local wedge protrusions to shadow flange joints. The lower DDBA dipole field of 0.8 T compared with the existing DBA dipole field of 1.4 T was helpful in reducing the SR heat load.

5 inverted magnetron cold-cathode gauges, shielded from scattered electrons and photons, were fitted for total pressure measurements along with 4 residual gas analysers (RGAs) for partial pressure measurements.

After extensive laboratory trials, spring-energised metal vacuum seals [7] were selected for flange joints along the electron beam path due to the need for low RF impedance, and hence low gap, joints. In production, the surface finish on the mating flanges in the seal region turned out to be critical and a number of iterations were needed before a satisfactory seal could be reliably obtained.

All vacuum vessels and components were baked out to 200 °C by the supplier and mechanically inspected before delivery as part of the factory acceptance tests.

BUILD AND INSTALLATION

The vessels were assembled on 2 steel girders in Diamond's Technical Support Building, pumped down and an initial bakeout was carried out at 200 °C for 48 h without any of the magnets in place. The vessels were then removed and set aside while the magnets were aligned on the girders. The quadrupole and sextupole magnets were then split, the magnet tops removed and the vessels fitted into the magnet lower halves. A second, final 48 h bakeout was then carried out; the temperature was limited to 180 °C to avoid overheating the magnet poles. On cool down, the vacuum equipment was degassed, the NEG cartridges were activated using a local power supply and the SIPs were powered up. The multipole magnets were then reassembled and the dipole magnets slid into space from the side.

The on-girder bakeouts were carried out using a custom designed PLC-controlled bakeout system. A combination

of low voltage DC Kapton thin film heaters and mains powered heater tapes and insulated heater jackets were used. The PLC system was able to control the temperature ramp up and ramp down as well as maintaining the programmed temperature within ± 10 °C along each of the girders.

It was the intention to install the girders in the storage ring without any further venting of the vacuum system. In practice however the vacuum system was vented several times during the installation process to correct some minor assembly issues. In each case venting was carried out using dry, high purity nitrogen. Although the vacuum system was capable of *in-situ* bakeout, it was decided not to carry out additional baking after venting as the vacuum recovered well over time without further baking.

BEAM CONDITIONING AND VACUUM PERFORMANCE

To enable direct comparison of simulations and measurements, published gauge sensitivity factors [8] combined with averaging over the 5 gauge positions, were used to reduce the simulated multi-gas pressure distribution to a single mean pressure. A similar average was taken for the measured total pressures at each of the same 5 gauge positions. Finally, before plotting, all the pressures were normalised by dividing by the beam current. N.B., due to the different weighting factors employed, these pressures are numerically different from the CO-equivalent pressures plotted in Figures 2 and 3.
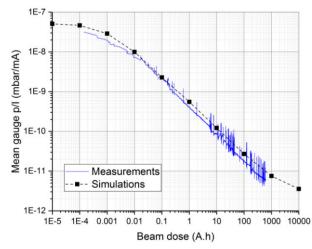

Figure 4: Comparison of measured and simulated pressure (as indicated on gauges) during beam conditioning.

Figure 4 shows the simulated and measured dynamic pressure, *vs* beam conditioning dose. It can be seen that there is excellent agreement between the simulations and measurements within a factor 2. After an initial curved portion the beam conditioning curve has a slope of -0.67. This is within the typical range of electron storage ring beam conditioning behaviour [6]. The residual gas is mainly hydrogen with only small amounts (<10% and decreasing with beam dose) of CO and other gases.

The measured beam lifetime (normalised by beam current) is shown *vs* beam conditioning dose in Figure 5. Up

to around 70 A.h the lifetime increases in inverse proportion to the decreasing pressure. At higher beam doses the pressure continues to decrease but the lifetime no longer increases significantly indicating that beam losses are no longer dominated by gas scattering. The jumps and spikes in lifetime are due to changes in machine operating conditions such as horizontal-vertical coupling, beam current and insertion device gaps.

The main contributors to the measured lifetime (τ) will be gas scattering (τ_{gas}) and intrabeam scattering ($\tau_{Touschek}$). τ_{gas} will be inversely proportional to pressure while $\tau_{Touschek}$ will be inversely proportional to beam current for a constant set of machine operating conditions [9].

This relationship is explored using the trace labelled "Fit" in Figure 5 which has the equation:

$$y\ (A.h)^{-1} = 0.3 + 2.10^9\ p_g/I\ (mbar/mA)$$

with parameters chosen for best fit to the observed beam lifetime. The first term represents $\tau_{Touschek}$ while the second term represents τ_{gas}. p_g is the mean gauge total pressure reading as described above. From this we can derive the following simple expression for the gas lifetime:

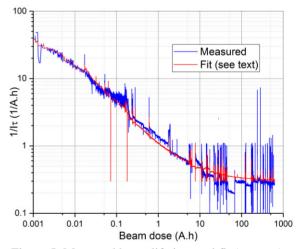$$\tau_{gas}\ (h) \approx 5.10^{-7}/p_g\ (mbar)$$

Figure 5: Measured beam lifetime and fit (see text).

REFERENCES

[1] R.P. Walker *et al.*, in *Proc. IPAC'16*, pp. 2953-2955.

[2] E. Al-Dmour *et al.*, in *Proc. IPAC'11*, pp. 1554-1556.

[3] CapaciTorr® D400-2, SAES Getters S.p.A.

[4] B.F. Macdonald *et al.*, "Storage ring vacuum system pressure modelling at Diamond", *Vacuum*, vol. 84, pp. 283-285, 2009.

[5] COMSOL Multiphysics®, COMSOL Inc.

[6] O. B. Malyshev and M. P. Cox, "Design modelling and measured performance of the vacuum system of the Diamond Light Source storage ring", *Vacuum*, vol. 86, pp. 1692-1696, 2012.

[7] Helicoflex® HN 100, Technetics Group.

[8] K. Jousten Ed., "Handbook of vacuum technology", Weinheim, Germany: Wiley-VCH, 2008.

[9] A. Wrulich, in *Proc. 5th General Accelerator Course*, pp. 409-435.